Myxoma Virus Leukemia-Associated Protein Is Responsible for Major Histocompatibility Complex Class I and Fas-CD95 Down-Regulation and Defines Scrapins, a New Group of Surface Cellular Receptor Abductor Proteins

Jean-Luc Guerin,[1] Jacqueline Gelfi,[1] Severine Boullier,[1] Maxence Delverdier,[2] Frederique-Anne Bellanger,[1] Stephane Bertagnoli,[1] Ingo Drexler,[3] Gerd Sutter,[3] and Frederique Messud-Petit[1]*

UMR 960 Microbiologie Moléculaire[1] and Laboratoire d'Anatomie-Pathologique,[2] Institut National de la Recherche Agronomique and Ecole Nationale Vétérinaire, 31076 Toulouse, France, and GSF—Institut für Molekulare Virologie/Institut für Virologie TUM, 81675 Munich, Germany[3]

Down-modulation of major histocompatibility class I (MHC-I) molecules is a viral strategy for survival in the host. *Myxoma virus*, a member of the *Poxviridae* family responsible for rabbit myxomatosis, can down-modulate the expression of MHC-I molecules, but the viral factor(s) has not been described. We cloned and characterized a gene coding for an endoplasmic reticulum (ER)-resident protein containing an atypical zinc finger and two transmembrane domains, which we called myxoma virus leukemia-associated protein (MV-LAP). MV-LAP down-regulated surface MHC-I and Fas-CD95 molecules upon transfection; the mechanism probably involves an exacerbation of endocytosis and was lost when the ER retention signal was removed. In addition, the lytic activity of MHC-I-restricted antigen-specific cytolytic T lymphocytes (CTL) against myxoma virus-infected antigen-presenting target cells was significantly reduced, revealing a strong correlation between MHC-I down-regulation by MV-LAP and CTL killing in vitro. In vivo experiments with a knockout virus showed that MV-LAP is a virulence factor, potentially involved in the immunosuppression characteristic of myxomatosis. Data bank analysis revealed that MV-LAP has homologs in herpesviruses and other poxviruses. We propose the name "scrapins" to define a new group of ER-resident surface cellular receptor abductor proteins. The down-regulation of cell surface molecules by scrapins probably helps protect infected cells during viral infections.**

Recognition of viral antigens by cytolytic T lymphocytes (CTL) is one of the most efficient ways to eliminate virus-infected cells. Their recognition occurs through the interaction between the T-cell receptor of a cytotoxic cell and a viral peptide bound to a class I major histocompatibility complex (MHC-I) molecule (31). Several mechanisms for interfering with MHC-I cell surface display have been developed by large DNA viruses (28). Basically, all the steps of the trafficking of MHC-I molecules and their association with peptides are targets of viral strategies: these can be the inhibition of transporter associated with antigen processing (TAP)-dependent peptide translocation from the cytoplasm to the endoplasmic reticulum (ER) (24); the accumulation of MHC-I in the ER, preventing the accession of assembled molecules to the cell surface (2); or the translocation of ER-resident MHC-I molecules to the cytosol and their subsequent degradation by proteasomes (46). Once the peptide-bound MHC-I molecules have reached the plasma membrane, they can be retrieved from the cell surface by viral products such as the Nef protein of human immunodeficiency virus (HIV) type I, which enhances their endocytosis (38).

Myxoma virus (MV), a member of the *Poxviridae* family, is the agent responsible for myxomatosis, a highly lethal disease of the European rabbit (*Oryctolagus cuniculus*) (14). MV has a double-stranded DNA of 162 kbp (9), with a central region containing highly conserved enzymatic and structural genes required for the maintenance of essential viral functions. Peripheral regions of the DNA, within and near the inverted terminal repeats (ITR) at both sides of the genome, encode nonessential factors that contribute to the modulation of the host response to infection (13, 42, 43).

Several MV proteins have been shown to be associated with virulence and immunomodulation (for a review, see reference 4). MHC-I down-regulation has been observed in MV, where one or several factors enhance the endocytosis of MHC-I molecules, leading to their degradation in endolysosomal compartments (6, 50). The viral factor(s) and underlying molecular mechanism(s) have not been described. In this paper, we identify MV leukemia-associated protein (MV-LAP) as a member of a new group of viral proteins containing a LAP plant homeodomain (LAP-PHD) motif and hydrophobic domains. Members of this group, tentatively named "scrapins," are ER proteins, encoded by large DNA viruses, which participate in the down-regulation of cell surface molecules involved in the immune response. We show that MV-LAP down-regulates the cell surface display of both MHC-1 and Fas-CD95 molecules, acting as a virulence factor important for virus pathobiology.

* Corresponding author. Mailing address: UMR 960 Microbiologie Moléculaire, Ecole Nationale Vétérinaire, 23, Chemin des Capelles, 31076 Toulouse, Cedex 3, France. Phone: 33 561 19 38 78. Fax: 33 561 19 39 74. E-mail: f.messudpetit@envt.fr.

MATERIALS AND METHODS

Cells, viruses, and transfections. The wild-type strain T1 and the MV-ΔLAP mutant of MV were grown on rabbit kidney cells (RK13) in OPTI minimal essential medium supplemented with 2% calf serum. Rabbit lymphocytes (RL5) were grown in RPMI 1640 supplemented with 5% calf serum. Strain T1 of MV is a field strain isolated in Toulouse, France, with a biology and a life cycle comparable to those of the Lausanne strain (8). For flow cytometry analysis, viruses were grown on baby green monkey kidney (BGMK) cells in Dulbecco's minimal essential medium with 2% calf serum. Subconfluent layers of BGMK cells were grown on glass coverslips and transfected with plasmids encoding green fluorescent protein (GFP) fusion proteins by using liposomes (Lipofectamine; Gibco BRL). At 24 h posttransfection, cells were rinsed twice with phosphate-buffered saline (PBS) for subsequent use in fluorescence-activated cell sorter (FACS) analysis or confocal microscopy.

The HLA-A2.1-positive human melanoma cell line Malme 3 M (ATCC HTB-64; HLA phenotype A2, Aw30, B13, B40+/−, DRw7) and the negative human melanoma cell line SK28-Mel-1 (ATCC HTB-72; HLA phenotype A11, A26, B40, DRw4) were used for FACS analysis and served as tyrosinase-expressing target cells in ^{51}Cr release assays. Cells were grown in RPMI 1640 supplemented with 10% heat-inactivated fetal calf serum (Seromed; Biochrome KG, Berlin, Germany) at 37°C in a humidified 5% CO$_2$ atmosphere.

The A2.1-restricted murine CTL lines specific for human tyrosinase peptide residues 369 to 377 (CTL A2Kb huTyr) or for influenza virus A/PR/8/34 matrix protein M1 peptide residues 58 to 66 (CTL CD8xA2Kb FluM1, which served as a negative control), as well as an alloreactive A2.1-specific murine CTL line (CTL CD8 allo A2.1), were established and maintained as described previously (12, 39). CTL were used as effector cells in 5-h ^{51}Cr release assays.

Cloning, sequencing, and computer analysis of DNA sequences. The viral DNA between the *serp-1* and *serp3* genes was amplified and sequenced as described previously (16). DNA sequences were analyzed using DNA Strider 1.3 software (26) and the BLAST program (GenBank). Edited sequences were analyzed with the GAP program package (SwissProt, release 33, March 1996). Multiple sequence alignments were performed by using ClustalW, consulted on the Network Protein Sequences Analysis browser (http://npsa-pbil.fr). Putative transmembrane (TM) domains were detected by using TMPRED software (http://www.ch.embnet.org/software/TMPRED).

Construction of GFP fusions. Fusion plasmids were obtained by subcloning specific MV-LAP fragments into the pEGFP plasmid vector (Clontech), which contains a jellyfish GFP gene optimized for maximum fluorescence downstream of a cytomegalovirus promoter. MV-LAP DNA comprising nucleotides (nt) 1 to 621, an N-terminal fragment (N-term-LAP) (nt 1 to 276), and a C-terminal fragment (C-term-LAP) (nt 283 to 621) were obtained by PCR using purified MV DNA as a template (35). PCR products were digested with the restriction enzymes *Nde*I and *Sma*I and cloned into the corresponding sites of pEGFP, yielding fusions containing GFP at the N terminus of the chimeric polypeptide. The integrity of MV fragments was assessed by sequencing.

Construction of MV-ΔLAP recombinant and revertant viruses. To evaluate the involvement of MV-LAP in MV pathogenicity, the *MV-LAP* gene was inactivated by deletion and disruption with the *lacZ* marker gene. Two sets of primers containing 5′-terminal extensions with restriction sites for subsequent subcloning were used to amplify fragments immediately upstream and downstream of the LAP domain. The primers were Serp3-sense (5′-CAGCAGCCCGGGTATGG ATATCTTTAATCATTTAAA-3′) paired with LAP-(antisense 60–40)-*Pst*I (5′-CAGCACTGCAGGCTTACATCGTCCAGGTTTAC-3′) and LAP-(sense 207–230)-*Xba*I (5′-CAGCTCTAGAGTCCGTACAACCTAAAGCGGC-3′) paired with LAP-(antisense 621–600) (5′-CAGCAAGCTTTCTAAGCGGGTGACTC CACGA-3′). After digestion with *Pst*I and *Xba*I, the fragments were cloned into a pGEM-T phagemid expression vector (Promega) upstream and downstream, respectively, of a *Pst*I-*Xba*I *lacZ* gene under the control of the vaccinia virus p7.5 promoter. The resulting plasmid, pMV-LAP::LacZ, thus consisted of an antisense *lacZ* gene replacing the LAP domain of MV-LAP. After pMV-LAP::LacZ was sequenced, it was used for transfection of MV-infected cells. MV-ΔLAP mutant viruses were screened by LacZ phenotype selection. PCR analysis of recombinant virus DNA was performed to confirm the absence of wild-type virus in preparations of MV-ΔLAP mutant virus. Finally, the absence of expression of MV-LAP in MV-ΔLAP-infected cells was assessed by reverse transcription-PCR (RT-PCR) analysis. A revertant virus, MV-LAP-*rev*, containing a wild-type MV-LAP open reading frame was obtained by transfecting plasmid DNA containing the complete *MV-LAP* gene into MV-ΔLAP-infected RK13 cells and by reverse white-blue screening.

Confocal microscopy observations. Cells were plated onto LabTek multichamber slide flasks (Nunc). At 24 h posttransfection the cells were incubated for 30 min at 37°C in 1 μM ER-Tracker (Molecular Probes, Leiden, The Netherlands) in culture medium, rinsed twice in PBS, fixed for 15 min at room temperature with 4% paraformaldehyde in PBS, and then counterstained with 50 μg of propidium iodide/ml–100 μg of RNase A/ml at room temperature for 30 min. After a final wash, the samples were mounted with PBS-glycerol (1:1) and observed with a confocal LSM Zeiss microscope fitted with a 63× Zeiss objective.

Flow cytometry analysis of transfected or infected cells. At 24 h posttransfection or 36 h postinfection (p.i.), adherent BGMK cells were detached by a 15-min incubation in PBS– 2 mM EDTA, rinsed in PBS–1% bovine serum albumin (BSA), and incubated with phycoerythrin-conjugated monoclonal antibodies (MAbs) to MHC-I, CD95, or CD71, or their respective isotype control antibodies (PharMingen Becton Dickinson), for 30 min at 4°C. After a wash, cells were analyzed by use of a FACScalibur (Becton Dickinson) and CELLQuest software.

Analysis of MHC-I cell surface expression on HLA-A2.1-positive Malme 3 M cells and HLA-A2.1-negative SK28-Mel-1 cells was performed 24 h after infection at a multiplicity of infection (MOI) of 10 with MV T1 or MV-ΔLAP. The cells were stained in PBS–1% BSA–1 μg of ethidium monoazidbromide (EMA) (Molecular Probes)/ml for 20 min at 4°C. The live or dead stained cells were washed and incubated either with hybridoma supernatants containing the anti-human HLA-A2.1 MAb BB7.2 (ATCC HB-82) or the anti-human HLA-A, -B, and -C MAb W6/32 (ATCC HB-95) or the respective isotype control IgG2b (PharMingen Becton Dickinson) or with immunoglobulin G2a (Dianova, Hamburg, Germany) as the first antibody. After a wash, the Fcγ fragment-specific F(ab′)$_2$ fragment of goat anti-mouse immunoglobulin G conjugated with fluorescein isothiocyanate (Dianova) was used as the secondary antibody for all cells. After three washes with PBS–1% BSA, FACS analysis was performed, excluding EMA-positive dead cells.

Chromium release assays. The lytic activity of the tyrosinase-specific CTL line (CTL A2Kb huTyr) or the alloreactive A2.1-specific murine CTL line (CTL CD8 allo A2.1) was tested against MV-T1-, MV-ΔLAP-, or mock-infected human melanoma target cells in a 5-h standard ^{51}Cr release assay. Briefly, Malme 3 M cells and SK28-Mel-1 cells were infected for 2 h at an MOI of 10, washed once, labeled for 1 h at 37°C with 100 μCi of Na^{51}CrO$_4$, and then washed four times. Labeled target cells were plated in U-bottom 96-well plates at 10^4 cells/well and incubated for an additional 20 h at 37°C. At 24 h p.i., effector cells were incubated with target cells at various effector/target ratios. After 5 h, 100 μl of supernatant per well was collected and the specific ^{51}Cr release was determined. Assays were performed in triplicate.

Single-step growth analysis of viruses. RK13 and RL5 cells were infected for 2 h with either MV strain T1 or MV-ΔLAP at an MOI of 5. Unadsorbed free virus was removed and replaced by growth medium. Cells were incubated at 37°C and harvested at multiple time points postinoculation. Virus was released by freeze-thawing and brief sonication. Virus titers in the lysates were determined by standard plaque titration on RK13 cell monolayers.

RNA extraction and RT-PCR analysis. RK13 cells (5×10^6) were infected at an MOI of 5 with wild-type strain T1 or MV-ΔLAP. Total RNA was isolated at 2, 4, 8, 12, and 16 h p.i. with TRIzol reagent (Gibco BRL) according to the manufacturer's instructions. In addition, total RNA was also extracted from infected cells treated with 40 μg of cytosine arabinoside (araC)/ml at the time of infection. For RT-PCR analysis, an *MV-LAP*-specific primer was used for cDNA first-strand synthesis, followed by PCR amplification using *MV-LAP*-specific primers, namely, *MV-LAP-Fwd-Bam*HI (5′-CAGCGGATCCGGTAAACATG GCTACTGTTG-3′) and *MV-LAP-Rev-Pst*I (5′-AAACTGCAGTTTCTAAGCG GGTGACTCCA-3′), corresponding to the 5′ and 3′ ends of the open reading frame, respectively.

Infection of rabbits with the MV-ΔLAP mutant virus. Eight-week-old male New Zealand White rabbits were obtained from a local supplier and housed in biocontainment facilities according to the guidelines of the European Community Council on Animal Care (European Council directive 86/609/ECC, 24 November 1986). All procedures on the animals were performed by workers accredited by the French Ministry of Agriculture and were aimed at limiting animal pain and distress. Infections were performed intradermally in the right ear with 5×10^3 PFU of either wild-type MV, MV-ΔLAP, or MV-LAP-*rev*. Rabbits were monitored daily for clinical signs of myxomatosis (14). Rabbits that became moribund were sacrificed with T61 (Distrivet) administered intravenously. For histological studies, six rabbits were inoculated with MV strain T1 and six were inoculated with MV-ΔLAP as described above. At 4, 8, and 12 days p.i., two animals from each group were sacrificed. Two mock-infected rabbits were sacrificed and used as controls.

Histological examination. All animals were subjected to a complete postmortem examination. Tissue material from the injection site (ear [primary site]) and parotid lymph node were taken and stored in 10% neutral formalin for further

analysis. After fixation, tissues were processed routinely into paraffin blocks, sectioned at a thickness of 4 μm, and stained with hematoxylin and eosin for microscopic examination. Histological lesions were assessed and graded as minimal, light, moderate, marked, or severe. The terminal deoxynucleotidyltransferase-mediated dUTP-biotin nick end labeling (TUNEL) method was used to assess apoptosis of lymphocytes in parotid lymph nodes as described elsewhere (29). The following form of grading, based on the number of apoptotic bodies for each microscopic field at a magnification of ×400, was used: 25 to 50 apoptotic bodies, minimal apoptosis; 50 to 75 apoptotic bodies, light apoptosis; 75 to 100 apoptotic bodies, moderate apoptosis; 100 to 125 apoptotic bodies, marked apoptosis; more than 125 apoptotic bodies, severe apoptosis.

Virus load in tissues. White blood cells, spleens, lungs, testes, and controlateral parotid lymph nodes were sampled from rabbits infected with either wild-type or MV-ΔLAP mutant virus at 4, 8, and 12 days p.i. and were frozen at −80°C; after thawing, tissues were further disrupted by Dounce homogenization in Dulbecco's minimal essential medium. Virus titers in the different samples were determined by standard plaque titration on RK13 cell monolayers.

Nucleotide sequence accession number. The nucleotide sequence and the deduced amino acid sequence of MV-LAP have been deposited in GenBank under accession number AF229033.

RESULTS

MV encodes a protein homologous to several gammaherpesvirus- and poxvirus-encoded factors. During systematic sequencing of the right end of the genome of MV, we had previously identified two genes encoding serpins, *serp2* (34) and *serp3* (16), near the ITR. We also identified an open reading frame of 621 bp, downstream of *serp3*, on the genome of MV strain T1, which is routinely used in our laboratory (Fig. 1A). This gene is closely related to the M153R and M153.1R open reading frames, described by the complete genome analysis of the Lausanne strain of MV (9). However, the M153R and M153.1R open reading frames were described as a split version of the S153R gene of Shope fibroma virus, another leporipoxvirus, due to a frameshift at codon 110. Surprisingly, we found that there is no frameshift in the corresponding gene of MV strain T1, leading to a putative polypeptide of 206 residues. The deduced amino acid sequence showed significant homology with cellular and viral zinc finger proteins referenced in the GenBank database. The zinc finger has a non-classical C_4HC_3 signature, corresponding to the LAP (37) or PHD family (1), and is referred to below as the "LAP domain." Two hydrophobic regions are located in the center of the protein and may correspond to TM domains. These features are shared by gammaherpesvirus proteins such as human herpesvirus 8 (HHV-8; also known as Kaposi's sarcoma-associated herpesvirus) K3 and K5 (30), bovine herpesvirus 4 IE-1A and IE-1B (44), murine gammaherpesvirus 68 IE-1 (45), and herpesvirus saimiri open reading frame 12 (3) (Fig. 1B). Among poxviruses, we found that Shope fibroma virus S153R (47), swinepox virus C7L (27), yaba-like disease virus (YLDV) 5L (22), and lumpy skin disease virus 010 (41) encode proteins with the same motifs (Fig. 1C).

Herpesvirus-encoded K3 and K5 are referred to as immediate-early proteins (30). Indeed, the TTTTTTTGT motif at the 3′ end of the MV gene, underlined in Fig. 1A, is reminiscent of the early termination signal of poxviruses (48). To assess the time course of MV-LAP gene expression, we detected MV-LAP mRNA by RT-PCR. MV-LAP mRNA was detected as early as 4 h p.i. and throughout the viral cycle, with a peak of expression at 12 h p.i. (Fig. 2). Blocking of intermediate and late gene expression with araC did not impair *MV-LAP* transcription, confirming that this gene is expressed at early times after infection, independently of DNA replication.

MV-LAP down-regulates the surface display of MHC-I and CD95 molecules in an ER retention dependent fashion and defines scrapins. To determine the localization of the protein, we tagged the complete or truncated forms of MV-LAP with N-terminal GFP. We expressed the tagged versions in RK13 cells, while staining them with an ER-specific dye. Transfected cells were examined by immunofluorescence using a confocal microscope. As shown in Fig. 3A, a reticular pattern of staining was observed with the MV-LAP–GFP fusion, reminiscent of the images obtained with K3 and K5 of HHV-8 (11, 17). Staining of the ER revealed an identical pattern (data not shown). The GFP tag was not responsible for ER retention, since a control GFP protein alone had a diffuse fluorescence, present in both the cytoplasm and the nucleus (Fig. 3B). To assess which domains are responsible for ER retention of MV-LAP, we constructed an N-term-LAP–GFP plasmid, expressing amino acids 1 to 94 (corresponding to the LAP domain without the TM domains) fused with GFP, and a C-term-LAP–GFP plasmid, expressing amino acids 95 to 206 (corresponding to the C-terminal and TM domains) fused with GFP. The subcellular localization of the N-term-LAP–GFP protein was diffuse in the cytoplasm and identical to that of the control GFP protein (Fig. 3C). The C-term-LAP–GFP protein was targeted to the ER, and its distribution matched that of the MV-LAP–GFP fusion protein (Fig. 3D). We conclude from these data that MV-LAP localization is reticular and dependent on the C-terminal part of the protein, which contains the TM domains.

Gammaherpesvirus K3 and K5 proteins can down-regulate the surface display of membrane-anchored molecules such as MHC-I (11, 19), intercellular adhesion molecule 1 (ICAM-1), and B7-2 (18). Other authors have independently described the loss of MHC-I antigens at the surfaces of MV-infected cells (6, 50). Hence, we investigated the biological properties of MV-LAP with respect to cell surface antigen expression. We performed flow cytometry analysis of MHC-I molecules at the surfaces of cells transfected with various GFP fusion proteins. Transfection of BGMK cells with an MV-LAP–GFP plasmid resulted in a specific down-regulation of MHC-I molecules at the surfaces of the cells (Fig. 4A). We performed the same experiment with CD95 antibodies, since CD95 cell surface display was not affected by K3 or K5 in HeLa cells, and therefore CD95 was considered a negative control (11). Surpris-


FIG. 1. Structures of scrapin genes and proteins. (A) Sequence of MV-LAP. The open reading frame corresponding to the protein is shown with amino acids in single-letter code below the DNA sequence. Star, stop codon; downward-pointing arrow, frameshift with the sequence published by Cameron et al. (9); underlined letters, early termination signal; boxed letters, C_4HC_3 (LAP) motif; shadowed letters, transmembrane domains. (B) C_4HC_3 (LAP) motif of viral scrapins. SFV, Shope fibroma virus; SPV, swinepox virus; BHV4, bovine herpesvirus 4; MHV68, mouse herpesvirus 68; HSV, herpesvirus saimiri. (C) General structure of viral scrapins. C_4HC_3, LAP motif; TM, transmembrane domain. Numbers above the diagrams, positions of amino acids flanking the LAP motifs; numbers on the right, lengths of the proteins.

A

```
nt                                                                                    aa
(-29)  GTCAATTAAAGTAAATAGGTTGTGTAAAC ATG GCT ACT GTT GTA AAC ATG GAC ACT GTT GTA AAC
                                     M   A   T   V   V   N   M   D   T   V   V   N    12

37     CTG GAC GAT GTA AGC CTG GCG GAT AAA TGT TGT TGG ATA TGC AAA GAA GCC TGT GAC ATC
        L   D   D   V   S   L   A   D   K   C   [C]  W   I  [C]  K   E   A   C   D   I   32

97     GTA CCC AAT TAC TGC AAA TGC CGA GGG GAT AAT AAG ATC GTG CAT AAG GAA TGT TTG GAA
        V   P   N   Y  [C]  K  [C]  R   G   D   N   K   I   V  [H]  K   E  [C]  L   E    52

157    GAG TGG ATC AAC ACA GAT GTC GTG AAA AAC AAA TCG TGT GCC ATA TGC GAG AGT CCG TAC
        E   W   I   N   T   D   V   V   K   N   K   S  [C]  A   I  [C]  E   S   P   Y    72

217    AAC CTA AAG CGG CGG TAC AAA AAA ATT ACC AAA TGG AGG TGT TAT AAA CGC GAC TGC CAC
        N   L   K   R   R   Y   K   K   I   T   K   W   R   C   Y   K   R   D   C   H    92
                                                                              ↓
277    GAT AGT TTA TTA GTA AAC ATG TCG CTT TGT TTG ATC GTG GGT GGA ATG GGG GGC TAT TTA
        D   S   L   L   V   N   M   S   L   C   L   I   V   G   G   M   G   G   Y   L   112

37     CTC ATT TCC ACG GAA ATT GTA AAA CTT ATA GCG TCT GAG GAA GTT AGC AAC ATT GCT AAA
        L   I   S   T   E   I   V   K   L   I   A   S   E   E   V   S   N   I   A   K   132

397    GTA TTT CTC GTC TCT GCG TCC ATG GGT CCA TTT ATG GTA TCC GCA TTA ACC ATG GTA CGT
        V   F   L   V   S   A   S   M   G   P   F   M   V   S   A   L   T   M   V   R   152

457    GCG TGT ATA GAC TGT CGT ACC TAC TTC ATA GCT ACT CGT GAA AAT ACG ATT CAC GAG
        A   C   I   D   C   R   T   Y   F   I   A   T   R   E   N   T   I   H   E   172

517    GTG GCA GAG ATG GAA GAT GTG GAG GAG GTG GAG GAG GTG AAC GAT GAC GAC GGC GAT GAA
        V   A   E   M   E   D   V   E   E   V   E   E   V   N   D   D   D   G   D   E   192

577    TAC GTC GAC GCT GTC GAG GAA ATC GTC GTG GAG TCA CCC GCT TAG AAAAACGAATCGAATAAAAA
        Y   V   D   A   V   E   E   I   V   V   E   S   P   A   *                        206

637    CCCGTGTACACACGGACGTTAATTTTTTTTTTGTGGGTTTAAAA
```

B

<u>poxvirus</u>
```
MV-MVLAP    CWICKEACDI-VPNYCKCRGDNKIVHKECLEEWINTDVVKNKSCAIC
SFV-153R    CWICKESCDV-VRNYCKCRGDNKIVHKECLEEWINTDTVKNKSCAIC
SPV-C7L     CWICKDDYSI-EKNYCNCKNEYKVVHDECMKKWIQYS--RERSCKLC
YLDV-5L     CWICNDVCDE-RNNFCGCNEEYKVVHIKCMQLWINYS--KKKECNLC
```

<u>herpesvirus</u>
```
BHV4-IE1A   CWICRDGESLPEARYCNCYGDLQYCHEECLKTWISMS--GEKKCKFC
BHV4-IE1B   CWICKGSEGIIDVKYCHCIGDLQYVHSECLVHWIRVS--GTKQCKFC
HHV8-K3     CWICNEELGNERFRACGCTGELENVHRSCLSTWLTIS--RNTACQIC
HHV8-K5     CWICREEVGNEGIHPCACTGELDVVHPQCLSTWLTVS--RNTACQMC
MHV68-IE1   CWICHQPEG-PLKRFCGCKGSCAVSHQDCLRGWLETS--RRQTCALC
HSV-ORF12   CLICCNIGEEELLQACDCPSR---VHHTCLQSHIQCF--KSSHCTFC
```

```
Consensus   C--C-----------C-C-------H--C--------------C--C
```
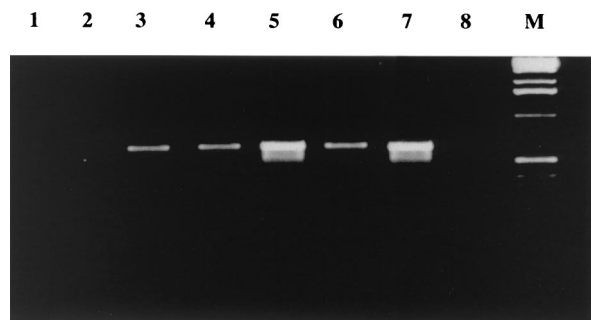
C

<u>poxvirus</u>

<u>herpesvirus</u>
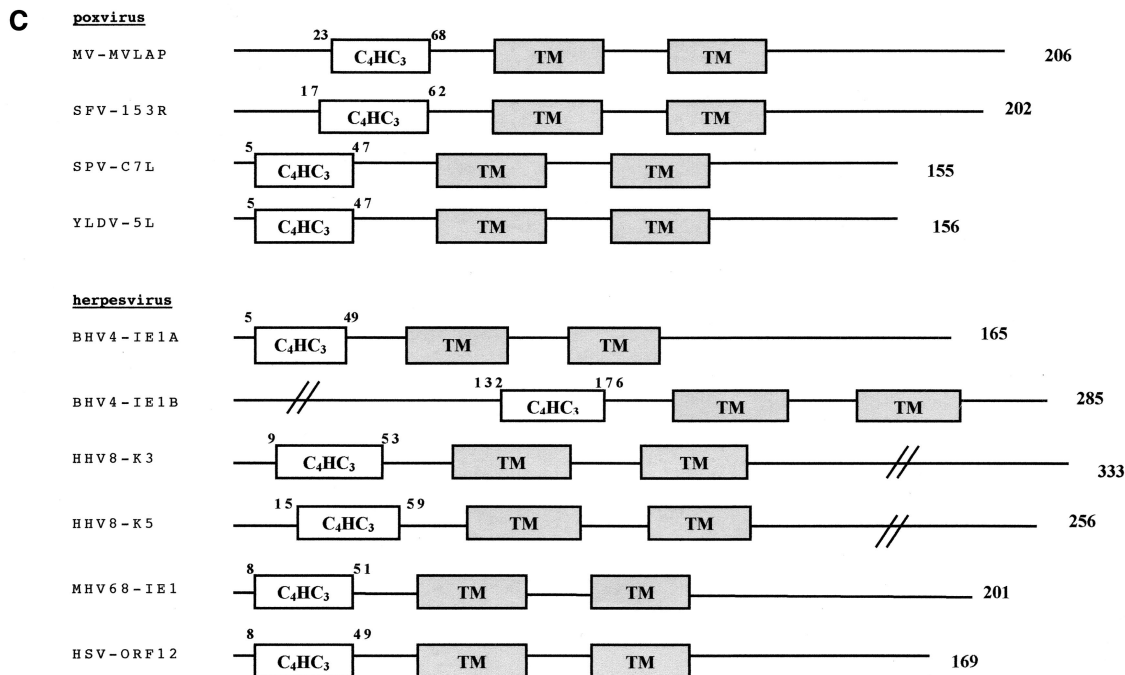
FIG. 2. Expression of MV-LAP mRNA in cell culture. mRNAs were extracted and subjected to RT-PCR using primers specific for *MV-LAP*. Lane 1, mock-infected cells; lanes 2 through 6, cells infected with wild-type MV for 2, 4, 8, 12, or 16 h, respectively; lane 7, cells infected with wild-type MV for 12 h and incubated with araC at the time of infection; lane 8, cells infected with MV-ΔLAP; lane M, marker.

ingly, transfection with MV-LAP–GFP reproducibly resulted in down-regulation of CD95, with a pattern similar to that of MHC-I down-regulation (Fig. 4B). Transferrin receptor (CD71) surface expression was unchanged after transfection with any of the constructs, confirming the specificity of MHC-I and CD95 down-regulation (Fig. 4C). To investigate the involvement of the reticular localization in this phenotype, we transfected BGMK cells with the N-term-LAP–GFP plasmid. Cells transfected with this truncated construct did not show any down-regulation of the surface display of MHC-I or CD95 molecules (Fig. 4), indicating that ER localization is necessary to this function.

Taken together, these results reveal that poxviruses and herpesviruses share structurally similar proteins that are involved in cell surface down-modulation of immune receptors. Members of this new group of proteins are retained in the ER, although they act through the abduction of cell surface mole-
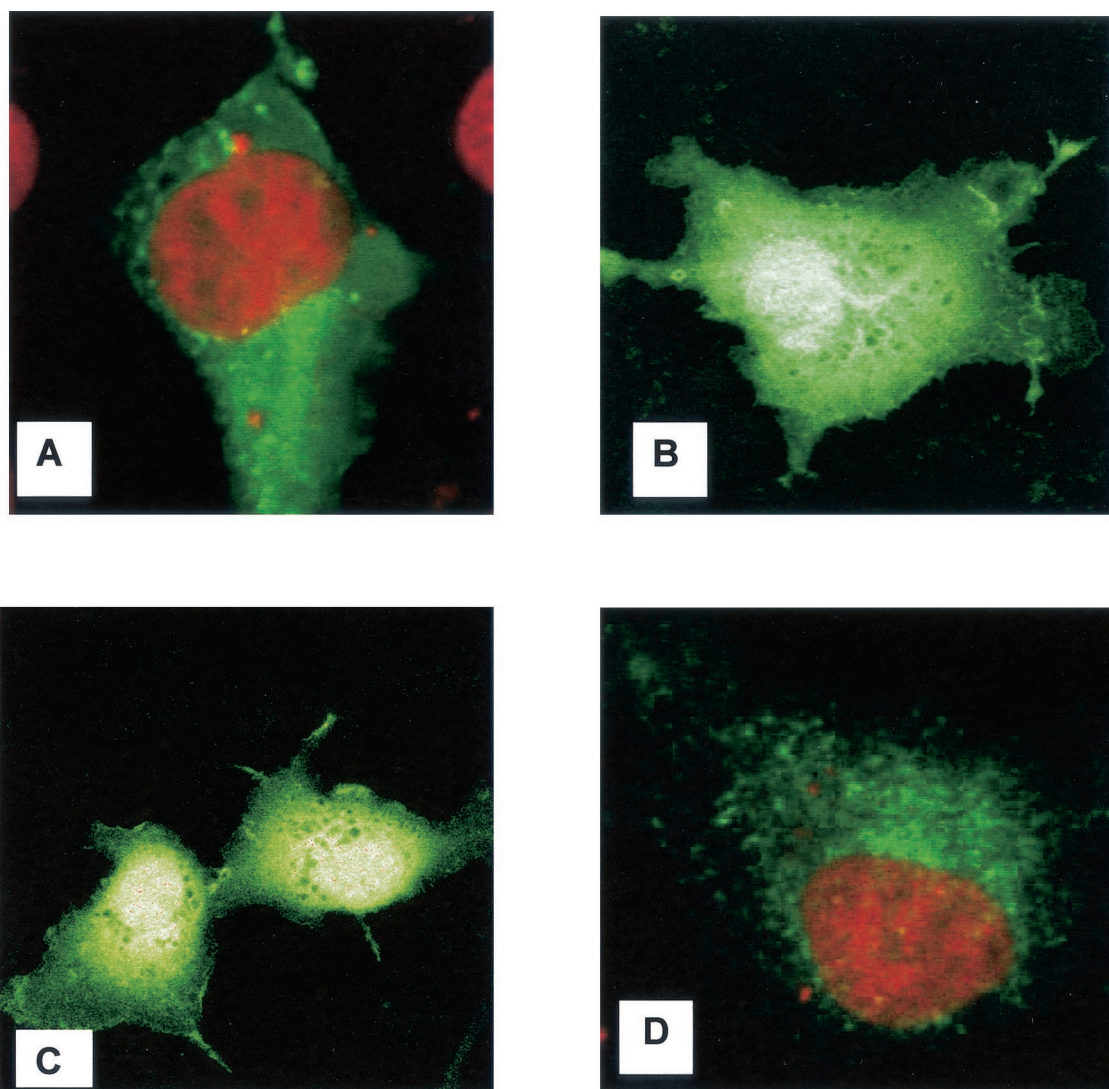

FIG. 3. Intracellular localization of MV-LAP. RK13 cells grown on coverslips were transfected with expression vectors for GFP-tagged versions of MV-LAP. Cells were fixed 36 h posttransfection, and nuclei were stained with propidium iodide (red in panels A and D; yellow upon merging with GFP as in panels B and C). (A) Full-length MV-LAP–GFP fusion; (B) GFP control; (C) N-term-LAP–GFP; (D) C-term-LAP–GFP.
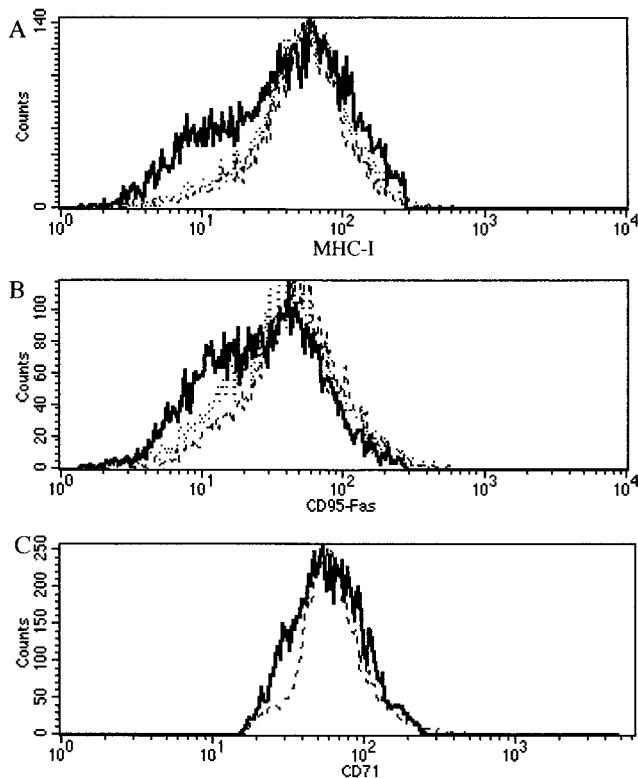
FIG. 4. Down-regulation of MHC-I and CD95 molecules in transfected cells. Transfected BGMK cells were gated for GFP fluorescence (FL-1) and were analyzed for MHC-I (A), CD95 (B), or CD71 (C) expression (FL-2). Transfections were performed with a GFP control plasmid (dashed lines; calculated medians, 52 for MHC-I, 42.4 for CD95, and 62.6 for CD71 expression), MV-LAP–GFP (bold lines; calculated medians, 38 for MHC-I, 27.4 for CD95, and 60.4 for CD71 expression), or N-term-LAP–GFP (dotted lines; calculated medians, 52.3 for MHC-I expression and 42 for CD95 expression). Background fluorescence revealed by staining with isotype control antibodies shows fluorescence in the first log. These data were reproduced in five independent experiments.

cules. We propose the name "scrapins" to refer to this family of surface cellular receptor abductor proteins.

Construction and characterization of an MV-ΔLAP mutant virus in cell cultures. The *MV-LAP* open reading frame is present as a single copy on the MV genome. To construct an MV-ΔLAP recombinant virus, we replaced the *MV-LAP* open reading frame of the T1 strain of MV with a *lacZ* marker gene under the control of the vaccinia virus p7.5 promoter, by homologous recombination. Because of the presence of the *Escherichia coli lacZ* gene within the genome of MV-ΔLAP mutants, isolation of viral foci from the background was facilitated by 5-bromo-4-chloro-3-indolyl-β-D-galactopyranoside (X-Gal) staining. We isolated an MV-ΔLAP mutant virus showing a LacZ phenotype. As a control, we constructed a revertant virus derived from MV-ΔLAP in which the complete *MV-LAP* open reading frame was restored by homologous recombination with a plasmid containing the whole *MV-LAP* gene. The resulting wild-type-like MV, designated MV-LAP-*rev*, was purified by several rounds of white-blue screening. To assess *MV-LAP* disruption, we analyzed MV-ΔLAP DNA by PCR with the specific primers *mv-lap-5′* and *mv-lap-3′*. No amplification

could be observed with MV-ΔLAP, in contrast with observations with the wild-type MV and revertant MV-LAP-*rev* DNAs (data not shown).

Single-step growth curve analysis showed no defects in the ability of MV-ΔLAP to replicate in RK13 cells. Similar results were obtained with a rabbit CD4$^+$ T-cell line (RL5). These results suggest that *MV-LAP* knockout does not alter the in vitro replicative capability of the virus.

We then assessed the effect of a viral infection on cell surface display of molecules. Infection of BGMK cells with MV strain T1 induced a significant decrease in MHC-I surface expression, contrasting with MV-ΔLAP and mock infections (Fig. 5A). CD95 expression was not affected by MV infection (Fig. 5B), suggesting additional pathways for CD95 regulation.

MHC-I down-regulation is associated with loss of CD8$^+$ T-cell-mediated cytotoxicity. In order to determine whether MHC-I down-regulation was associated with a functional defect, we tested the cytotoxic activity of a tyrosinase-specific HLA.A 2.1-restricted CTL line (CTL A2Kb huTyr) against melanoma target cells. Malme 3 M cells as well as SK28-Mel-1 melanoma cells are positive for the tumor antigen tyrosinase, but only Malme 3 M cells can present the tyrosinase peptide comprising amino acids 369 to 377 within the context of HLA-A2.1. We first checked whether MV infection induced MHC-I down-regulation on melanoma cells. Using a pan-HLA-A, -B, and -C MAb (W6/32), we observed a dramatic decrease in MHC-I cell surface expression 24 h after MV infection (3.34% W6/32-positive cells versus 99.8% for mock infection) (Fig. 6A). This decrease did not occur when Malme 3 M cells were
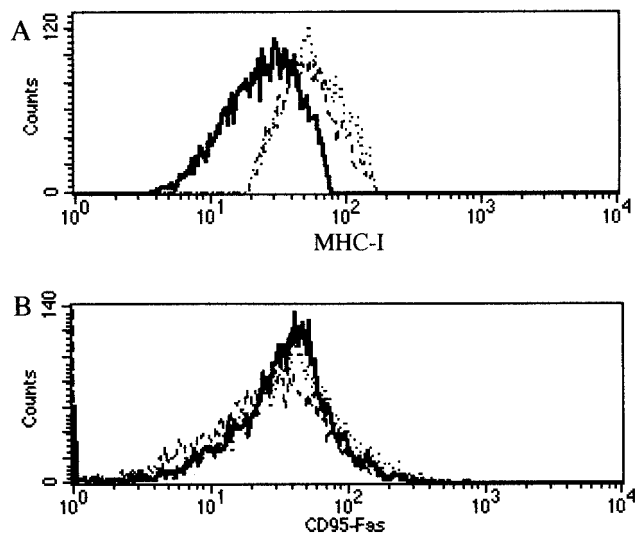

FIG. 5. MV-LAP affects MHC-I expression in infected cells. BGMK cells were analyzed for MHC-I (A) or CD95 (B) expression (FL-2). Cells were either mock infected (dashed lines; calculated medians, 50.6 for MHC-I expression and 36.4 for CD95 expression) or infected with either wild-type MV (bold lines; calculated medians, 24.6 for MHC-I expression and 35.4 for CD95 expression) or an MV-ΔLAP mutant virus (dotted lines; calculated medians, 54.2 for MHC-I expression and 37.8 for CD95 expression). Background fluorescence revealed by staining with isotype control antibodies shows fluorescence in the first log. These data were reproduced in five independent experiments.
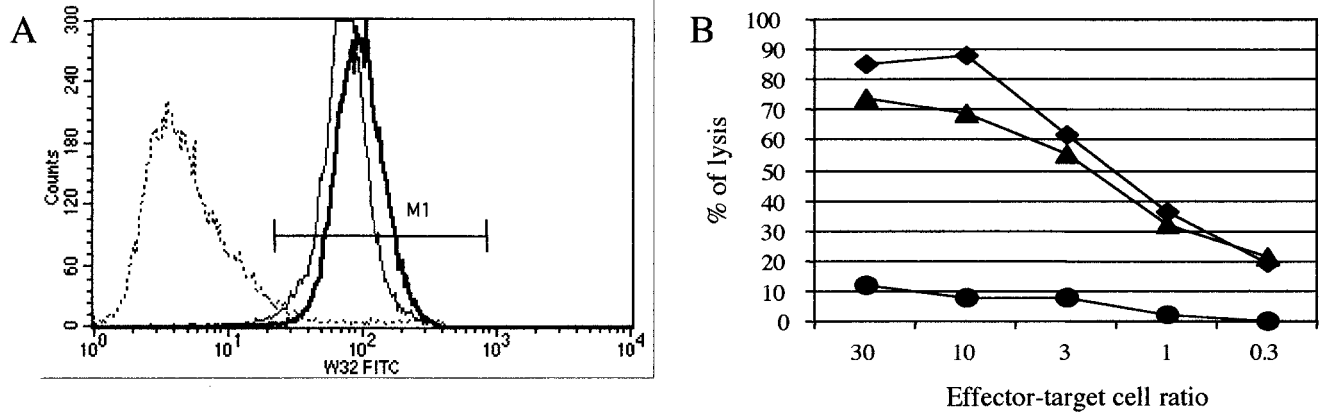
FIG. 6. MV-LAP expression affects both MHC-I expression and CTL lysis. (A) MV-LAP induces MHC-I down-regulation of Malme 3 M cells. Malme 3 M cells were either mock infected (solid line) or infected with either wild-type MV (dashed line) or an MV-ΔLAP mutant virus (bold line). Twenty-four hours postinfection, MHC-I surface expression was quantified using an anti-HLA-A, -B, and -C MAb. M1 represents the MHC-I-positive cell population. (B) Cytotoxic activity is abolished after MV infection. The lytic activity of the A2Kb huTyr CTL line was tested against mock-infected (diamonds), MV-infected (circles), and MV-ΔLAP-infected (triangles) Malme 3 M cells at the indicated effector/target cell ratios. Specific lysis was dramatically decreased after MV infection and almost unchanged after MV-ΔLAP infection.

infected with MV-ΔLAP (99.9% W6/32-positive cells). We obtained similar results on MHC-I down-regulation for SK28-Mel-1 cells (data not shown). Since the cytotoxic activity of A2Kb huTyr is HLA2.1 restricted, we also confirmed MV-induced down-regulation of HLA2.1 molecules on Malme 3 M cells by FACS analysis using an anti-HLA2.1 specific MAb (BB7.2) (data not shown). We then tested the effect of MHC-I down-regulation on cytotoxicity. Briefly, Malme 3 M and SK28-Mel-1 cells either were infected with either MV or MV-ΔLAP or were mock infected; then they were labeled with ^{51}Cr. Twenty-four hours later, the cytotoxic activity of CTL A2Kb huTyr against these targets was quantified. For Malme 3 M cells, we observed strong cytotoxic activity of effector cells against mock-infected cells, while cytotoxic activity against MV-infected cells was strongly reduced. In addition, CTL A2Kb huTyr killed MV-ΔLAP-infected cells as efficiently as it killed mock-infected cells (Fig. 6B). To ascertain that the inhibition of CTL activity was specific for MHC-I down-regulation, we also used an alloreactive A2.1-specific murine CTL line. A similar decrease in cytotoxic activity against MV-in-

fected cells was observed, while lysis activity against MV-ΔLAP-infected cells was unimpaired (data not shown). As anticipated, there was no lysis of target cells by CTL CD8xA2Kb FluM1, which is also HLA-A2.1 restricted but is directed against an irrelevant influenza virus matrix peptide epitope. SK28-Mel-1 targets were not recognized by any of the CTL lines, as expected (data not shown). These results demonstrate that MHC-I down-regulation induced by MV is associated with loss of CTL activity against infected target cells.

MV-LAP is a virulence factor in the European rabbit. To evaluate the role of MV-LAP in the pathobiology of MV, European rabbits were inoculated intradermally with either MV strain T1, MV-LAP-*rev*, or MV-ΔLAP. The clinical course was examined daily for 28 days. There was a marked reduction in the virulence of MV-ΔLAP compared to that of wild-type MV in rabbits (Table 1).

Until day 7 p.i., all three groups of rabbits suffered from typical signs of myxomatosis: all animals, whatever the virus, had developed a lesion at the inoculation site (primary myxoma) and secondary myxomas on the face and ears. They also

TABLE 1. Pathogenicity of MV-LAP in European rabbits

Day	Procedure or result	
	Wild type MV and MV-LAP-*rev*[a]	MV-ΔLAP mutant[b]
0	Intradermal inoculation of four rabbits with 5,000 PFU of the wild-type MV strain T1 and of four rabbits with 5,000 PFU of MV-LAP-*rev*	Intradermal inoculation of 12 rabbits with 5,000 PFU
4	Primary lesions at inoculation sites: soft, congested, ca. 1 cm	Primary lesions at inoculation sites: soft, congested, ca. 1.5 cm
7	Primary myxomas large and diffused. Gram-negative bacterial infections of nasal and conjunctival mucosa. Multiple secondary myxomas on face and ears; edema of the testicles.	Primary myxomas large and diffused. Gram-negative bacterial infections on nasal and conjunctival mucosa. Secondary myxomas on face and ears; edema of the testicles.
12	Multiple secondary myxomas turning necrotic. Dyspnea; severe infection of respiratory tract. Emaciated; prostrated. Severe inflammation of the testicles. All rabbits sacrificed because of increased severity of symptoms.	Few secondary myxomas, mostly on eyelids. Moderate to severe infection of respiratory tract. Mild inflammation of the testicles.
14		4/12 rabbits sacrificed
21		Decrease in respiratory signs; 8/12 rabbits recover and are sacrificed at day 28

[a] Rabbit survival: 0 of 4 and 0 of 4.
[b] Rabbit survival: 8 of 12.

TABLE 2. Histological observations of lesions from rabbits infected with wild-type MV or the MV-ΔLAP mutant virus

Site and symptom(s)	Lesion intensity (topography)[a] with the indicated virus at:					
	Day 4 p.i.		Day 8 p.i.		Day 12 p.i.	
	Wild-type	MV-ΔLAP	Wild-type	MV-ΔLAP	Wild-type	MV-ΔLAP
Primary[b]: perivascular dermatitis with						
Edema	++ (f)	++ (f)	+++ (d)	++	++++ (d)	+++
Heterophils	++ (s)	++ (s)	+++	++ (s)	++++	++ (s)
Mononuclear cells				+ (s)	+	+++
Secondary[c]						
Parotid node: lymphadenitis with						
Paracortical hyperplasia	++	++	++++	+++	++++	+++
Sinusal histiocytosis	++	++	++++	+++	++++ (e)	+++
Infiltration by heterophils	++	++	++++	+++	++++ (e)	+++
Spleen						
Lymphoid hyperplasia of periarteriolar sheaths	++	++	++	++	++	++
Infiltration by heterophils	++	++	++	++	++	++
Lungs						
Bronchointerstitial pneumonia	++ (f)	++ (f)	+	+	−	−
Heterophils around bronchioles	++ (s)	++ (s)	+ (s)	+ (s)	−	−
Hyperplasia of BALT	++	++	+	+	−	−

[a] Lesion intensity: +, minimal; ++, light; +++, moderate; ++++, marked. Lesion topography: s, scattered; f, focal; d, diffuse; e, extensive.
[b] Samples were taken from lesions at the inoculation site.
[c] Samples were taken from parotid nodes, spleens, and lungs.

suffered from moderate respiratory infections and were less active.

At day 12 p.i. the distribution of secondary lesions was different: whereas the rabbits inoculated with the wild-type MV had developed multifocal secondary myxomas, animals who had been injected with the MV-ΔLAP mutant had fewer secondary myxomas, which were restricted to the face and ears. Additionally, rabbits infected with the MV or MV-LAP-*rev* virus had developed infections of the respiratory tract and were euthanized for ethical reasons. All the animals that had received the MV-ΔLAP mutant suffered from moderate to severe respiratory infections, but they were far less prostrated and emaciated than wild-type virus-infected rabbits. Four rabbits had to be sacrificed between days 14 and 21, due to the severity of the symptoms; the other rabbits recovered completely within 28 days. The overall mortality rate of animals infected with the MV-ΔLAP virus was about 30%, in contrast with the typical 100% lethality of MV infection.

To summarize, our clinical observations revealed that infection with an MV-ΔLAP mutant virus induced a reduction in the distribution of secondary cutaneous myxomas and milder respiratory infections, resulting in a higher rate of recovery (over 70%), compared to a systematically fatal evolution after infection with wild-type MV.

Histological analysis of lesions and apoptosis from MV- and MV-ΔLAP-infected rabbits. All animals were subjected to complete postmortem examinations, and the results are reported in Table 2. Between day 4 and day 8 p.i., both groups showed the same pattern of lesions, including a light and focal bronchointerstitial pneumonia, a few heterophils around some bronchioles and in adjacent alveoli, and a light hyperplasia of bronchus-associated lymphoid tissue (BALT). At day 12 p.i., the site of injection (primary myxoma) showed some differences. In rabbits infected with wild-type MV, the inflammatory reaction consisted of perivascular dermatitis with marked edema, interstitial mucinosis, activated fibroblasts, marked in-

filtration by heterophils, and a minimal infiltration by mononuclear cells (lymphocytes, plasmocytes, macrophages). In rabbits inoculated with the MV-ΔLAP mutant, the edema was moderate and the infiltration by heterophils was light, contrasting with a moderate infiltration by mononuclear cells (Fig. 7). In the parotid lymph nodes the lesions were similar: marked lymphadenitis with paracortical lymphoid hyperplasia, extensive sinusal histiocytosis, and infiltration by multinucleated giant cells. The spleens of all groups showed a light lymphoid hyperplasia of periarteriolar sheaths and a light infiltration by heterophils in red pulp, as observed at days 4 and 8 p.i. The histopathological lesions of the lungs were resolved.

Since CD95 is involved in the induction of apoptosis, the TUNEL method was used to assess apoptosis of lymphocytes in the parotid lymph node. Lymphocytes from rabbits inoculated with either type of virus showed apoptosis comparable to that for the controls, and at the same level and localization (data not shown), indicating that MV-LAP has no influence on in vivo apoptosis of lymphocytes.

From these observations we conclude that infection by either virus resulted in early histopathological lesions of light and focal bronchointerstitial pneumonia in lungs but that these were temporary and resoluble; the major difference lay in the evolution of the inflammatory process at the primary site of infection, where at day 12 p.i. a marked infiltration by heterophils (i.e., neutrophils) was characteristic of infection with wild-type MV, while the inflammatory reaction progressed more rapidly and consisted mostly of mononuclear cells in lesions induced by the MV-ΔLAP mutant.

Viral replication in vivo. To ascertain that the differences in the clinical course of the disease and the histological findings between the two viruses were not associated with an impairment of the ability of MV-ΔLAP to replicate in vivo, we measured viral loads in the parotid lymph nodes, lungs, spleens, testes, and white blood cells at days 2, 4, 8, and 12 p.i. No significant difference could be found in any tissue or in white
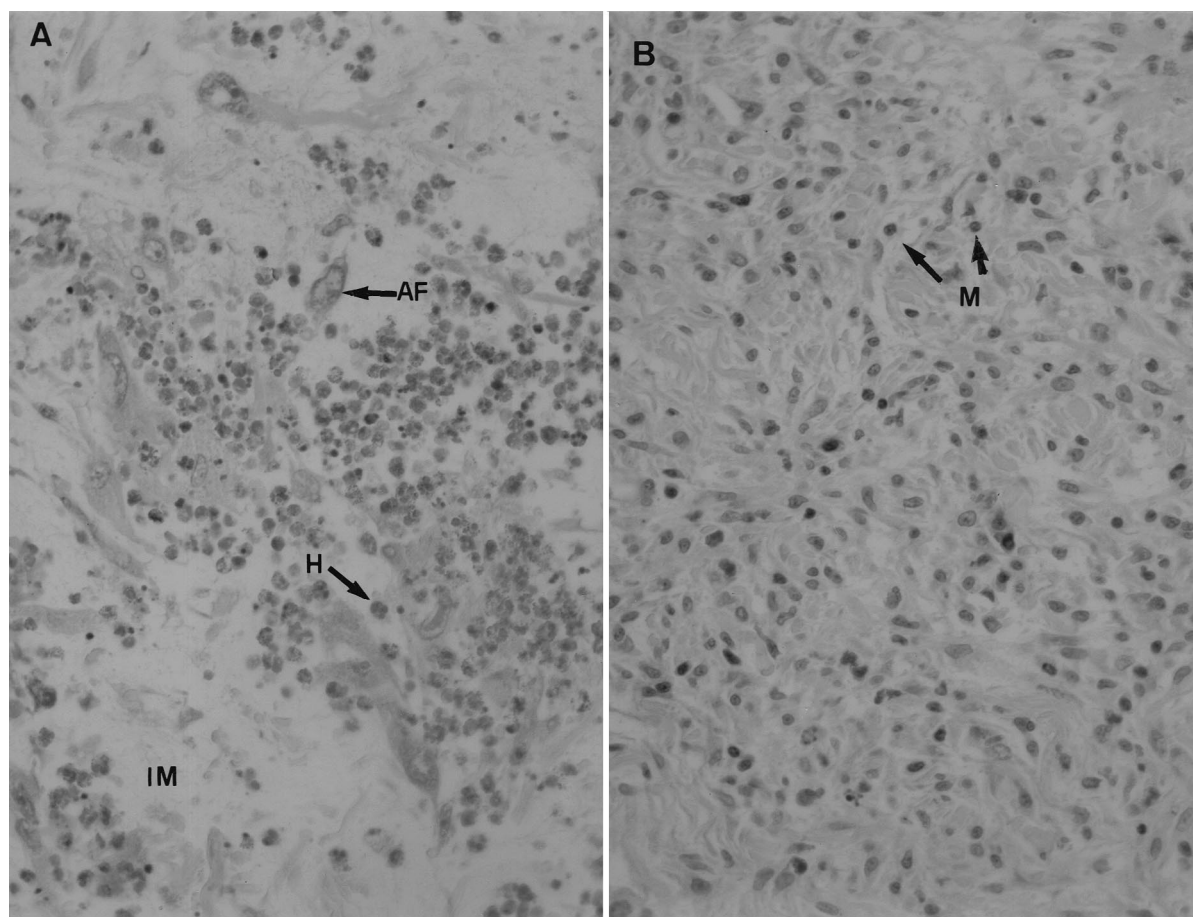
FIG. 7. Hematoxylin-and-eosin-stained skin samples (site of infection) from rabbits at 12 days postinoculation. Magnification, ×320. (A) Marked infiltration by activated fibroblasts (AF) and heterophils (H), and interstitial mucinosis (IM), with wild-type MV. (B) Mononuclear cells (M) are predominant in lesions induced by the MV-ΔLAP mutant.

blood cells (data not shown). We thus conclude that the ability of the MV-ΔLAP virus to replicate in vivo is not affected, and we cannot explain the observed attenuated phenotype.

DISCUSSION

While cell surface MHC-I down-regulation by MV has been reported, no molecular mechanism has yet been described (6, 49, 50). Here we were able to demonstrate that MHC-I down-regulation requires the expression of a viral gene encoding a protein homologous to cellular LAP (37) or the PHD family of proteins. This newly identified poxvirus factor was thus named MV-LAP. MV-LAP contains at least two domains, an atypical N-terminal ring finger, C_4HC_3—designated the LAP domain—and a cluster of two TM domains. These domains have been described for the herpesvirus proteins K3 and K5 of HHV-8 (11, 18, 19). We identified the same domains in proteins from other poxviruses, encoded by the Shope fibroma virus S153R (47), swinepox virus C7L (27), YLDV 5L (22), and lumpy skin disease virus 010 (41) genes. Hence, MV-LAP allows the identification of a group of proteins encompassing herpesviruses and poxviruses. This family consists of proteins with similar structures and functions; the latter suggest the name scrapins, which stands for surface cellular receptor abductor proteins.

Our results indicate that MV-LAP mRNA is expressed early in cell cultures, in accordance with previous observations that DNA replication inhibitors such as araC have no effect on MHC-I down-regulation in MV-infected cells (50). Furthermore, the pattern of MHC-I degradation appears as a progressive and cumulative process (50), in agreement with the persistence of MV-LAP expression during the whole viral cycle. All scrapins identified so far are indeed early gene products.

We could also show that MV-LAP reduces the surface display of CD95 molecules in vitro in a significant and specific manner, since the level of another membrane marker, CD71, was not affected by MV-LAP expression. However, in the course of a viral infection, the level of CD95 molecules was not affected. It is possible that another viral or virus-induced factor counteracts the action of MV-LAP with respect to CD95 regulation. A recent paper reporting that infection with a parapoxvirus increases CD95 mRNA expression (21) supports this hypothesis. Alternatively, CD95 turnover in the infected cell might be enhanced, thus masking the effect of MV-LAP.

Importantly, we could demonstrate in vitro that MV-LAP-mediated MHC-I down-regulation resulted in a dramatic decrease in MHC-I-restricted CTL activity against MV-infected human target cells. This finding strongly suggests that MV-

LAP function may potently interfere with MV-specific CD8^{+} T-cell (CTL) host responses and may represent a key factor for in vivo immune evasion by MV. Selective down-regulation of MHC-I proteins by viruses has been proposed as a viral strategy to allow for escape from CTL but avoid recognition by natural killer (NK) cells (10). While we observed a nearly complete down-regulation of MHC-I surface expression on MV-infected human melanoma cells, it should be noted that the melanoma cell lines used do not express HLA-C and that we did not monitor for HLA specificities other than HLA-A, -B, and -C. Therefore, it remains to be determined whether MV-LAP can down-regulate MHC-I proteins in a locus-specific manner as a possible mechanism for escape from NK lysis.

MV-LAP could down-regulate MHC-I expression on Malme 3 M cells even more efficiently than on BGMK cells. The latter is a monkey cell line for which the human anti-MHC-I antibody we used might have less affinity than it has for Malme 3 M cells, which are of human origin. Another explanation might lie in differential MHC-I expression between the two cell lines. Malme 3 M cells do not express HLA-C. It has been demonstrated that the intracytoplasmic tail of HLA-C is different from HLA-A and HLA-B tails and that HIV Nef induces HLA-A and -B down-regulation but is unable to down-regulate HLA-C because it cannot recognize its intracytoplasmic tail (23). A similar mechanism might exist for MV-LAP, and the down-regulation of MHC-I on BGMK cells would be less important because HLA-C levels would not be decreased. However, since no data are available concerning HLA display on BGMK cells, at this point this hypothesis can only be speculative.

Transfection experiments using an MV-LAP–GFP fusion construct revealed that MV-LAP is an ER protein, as deletion of the TM domains and the remaining C-terminal portion of the protein prevents it from residing in the ER. There is usually an easily identified consensus motif (KKXX or KXKXX) in the cytoplasmic domain of TM proteins that is responsible for their retention in the ER (20). Such a consensus could not be identified in MV-LAP. TM domains have been reported to contain ER localization signals (15). Hence, it is likely that the two TM domains of MV-LAP are responsible for its ER retention, although one cannot exclude the participation of some cryptic motif at the C terminus of the protein. MHC-I and CD95 down-regulation is abrogated when MV-LAP is not retained in the ER. Whether there is a direct relationship between ER localization and function is currently under investigation.

The Lausanne strain that was used in initial experiments (6, 50) is reported to have a frameshift at codon 110 (9), thus deleting the two TM domains. Since the absence of TM domains is hardly compatible with MHC-I down-regulation, we decided to sequence both strands of the corresponding region in the Lausanne strain as well. Our findings revealed that there is actually no frameshift in the Lausanne strain (data not shown). The most likely explanation is an error in the sequence published by Cameron et al. (9), since the frameshift occurs at a GGGGGG stretch (Fig. 1). Of course, there is still a remote possibility that the Lausanne strain sequenced by Cameron et al. actually possesses an additional G, in which case some other gene product might replace MV-LAP in MHC-I endocytosis.

The mechanism by which MV induces MHC-I down-regu-lation has been described as an enhanced endosomal/lysosomal retention, since it could be abolished by ATPase inhibitors such as NH_4Cl and leupeptin (50); similarly, K3 and K5 affect MHC-I display through the endocytosis of MHC-I molecules (11, 19). How can the ER localization of scrapins be reconciled with the degradation of membrane molecules? One hypothesis suggests a physical interaction between K5 of HHV-8 and cellular filamins (18). That would help explain how K5 can also down-modulate ligands such as ICAM-1 and B7-2, since the trafficking of all those molecules within the endosomal system involves the actin cytoskeleton. MV-LAP induces the internalization of MHC-I and CD95 molecules, both of which are membrane proteins that connect to the actin cytoskeleton via adapter molecules such as ezrin, furin, or filamin (25, 32). Interactions of MV-LAP with such tethers of the cytoskeleton have not been demonstrated yet but are being intensively studied in our laboratory.

Our model virus helped determine the role of scrapins in the pathobiology of viral infections—which cannot be achieved with human herpesvirus infections for obvious ethical reasons. To assess the role of MV-LAP in the pathogenesis of myxomatosis, we engineered a fully replication competent MV mutant with a deletion in the MV-LAP open reading frame. Although the mutant and wild-type viruses seem to replicate at the same level in vivo, the former induced fewer secondary lesions and milder respiratory infections, resulting in an impressively higher rate of recovery of the infected animals. Detailed histological examination could not explain the clinical differences, since lesions in the lungs were, surprisingly, very moderate in all cases. The only difference was observed at the site of infection, where the inflammatory response with the MV-ΔLAP mutant proceeded to the cellular phase (with lymphocytes and histiocytes infiltrating the lesion); in contrast, it was typically arrested at the vascular level upon inoculation with wild-type MV (29). The global decrease in the number of lymphocytes observed with the wild-type virus might reflect a milder infiltration of CD8 lymphocytes resulting from MHC-I down-regulation by MV-LAP. However, no tools are available yet to specifically identify rabbit CD8 lymphocytes in vivo. Since CD95 down-regulation could influence apoptosis of infected cells, we also investigated the level of apoptosis in the lymph nodes. Our observations indicate that the wild-type virus, as well as the MV-ΔLAP mutant, induces no significant apoptosis of lymphocytes. This is an indirect confirmation that CD95 is not affected by MV infection, suggesting the intervention of some factor that balances the action of MV-LAP and helps maintain a "physiological" level of CD95 molecules.

By allowing the virus to evade the host immune system, down-regulation of receptor molecules is a key feature of viral sabotage. It is particularly important to acknowledge the role of poxvirus scrapins in MHC-I down-regulation, since poxviruses are commonly used as vectors for foreign antigens (5, 7, 33, 36, 40). Indeed, it would be worth comparing viruses with deletions in the scrapin genes with their wild-type parents for the ability to induce a cellular immune response; the latter are probably less efficient at presenting antigens and thus make poorer vaccines.

REFERENCES

1. **Aasland, R., T. J. Gibson, and A. F. Stewart.** 1995. The PHD finger: implications for chromatin-mediated transcriptional regulation. Trends Biochem. Sci. **20:**56–59.
2. **Ahn, K., T. H. Meyer, S. Uebel, P. Sempe, H. Djaballah, Y. Yang, P. A. Peterson, K. Fruh, and R. Tampe.** 1996. Molecular mechanism and species specificity of TAP inhibition by herpes simplex virus ICP47. EMBO J. **15:**3247–3255.
3. **Albrecht, J. C., J. Nicholas, D. Biller, K. R. Cameron, B. Biesinger, C. Newman, S. Wittmann, M. A. Craxton, H. Coleman, B. Fleckenstein, et al.** 1992. Primary structure of the herpesvirus saimiri genome. J. Virol. **66:**5047–5058.
4. **Alcami, A., and G. L. Smith.** 1995. Cytokine receptors encoded by poxviruses: a lesson in cytokine biology. Immunol. Today **16:**474–478.
5. **Bertagnoli, S., J. Gelfi, G. Le Gall, E. Boilletot, J. F. Vautherot, D. Rasschaert, S. Laurent, F. Petit, C. Boucraut-Baralon, and A. Milon.** 1996. Protection against myxomatosis and rabbit viral hemorrhagic disease with recombinant myxoma viruses expressing rabbit hemorrhagic disease virus capsid protein. J. Virol. **70:**5061–5066.
6. **Boshkov, L. K., J. L. Macen, and G. McFadden.** 1992. Virus-induced loss of class I MHC antigens from the surface of cells infected with myxoma virus and malignant rabbit fibroma virus. J. Immunol. **148:**881–887.
7. **Boursnell, M. E. G.** 1992. Avipoxvirus vectors, p. 269–284. *In* M. M. Binns and G. L. Smith (ed.), Recombinant poxviruses. CRC Press, Boca Raton, Fla.
8. **Bouvier, G.** 1954. Quelques remarques sur la myxomatose. Bull. Off. Int. Epizoot. **46:**76–77.
9. **Cameron, C., S. Hota-Mitchell, L. Chen, J. Barrett, J. X. Cao, C. Macaulay, D. Willer, D. Evans, and G. McFadden.** 1999. The complete DNA sequence of myxoma virus. Virology **264:**298–318.
10. **Cohen, G. B., R. T. Gandhi, D. M. Davis, O. Mandelboim, B. K. Chen, J. L. Strominger, and D. Baltimore.** 1999. The selective downregulation of class I major histocompatibility complex proteins by HIV-1 protects HIV-infected cells from NK cells. Immunity **10:**661–671.
11. **Coscoy, L., and D. Ganem.** 2000. Kaposi's sarcoma-associated herpesvirus encodes two proteins that block cell surface display of MHC class I chains by enhancing their endocytosis. Proc. Natl. Acad. Sci. USA **97:**8051–8056.
12. **Drexler, I., E. Antunes, M. Schmitz, T. Wolfel, C. Huber, V. Erfle, P. Rieber, M. Theobald, and G. Sutter.** 1999. Modified vaccinia virus Ankara for delivery of human tyrosinase as melanoma-associated antigen: induction of tyrosinase- and melanoma-specific human leukocyte antigen A*0201-restricted cytotoxic T cells in vitro and in vivo. Cancer Res. **59:**4955–4963.
13. **Drillien, R., D. Spehner, D. Villeval, and J. P. Lecocq.** 1987. Similar genetic organization between a region of fowlpox virus DNA and the vaccinia virus *Hind*III J fragment despite divergent location of the thymidine kinase gene. Virology **160:**203–209.
14. **Fenner, F., and F. Ratcliff.** 1965. Myxomatosis. Cambridge University Press, Cambridge, United Kingdom.
15. **Fu, J., G. Pirozzi, A. Sanjay, R. Levy, Y. Chen, C. De Lemos-Chiarandini, D. Sabatini, and G. Kreibich.** 2000. Localization of ribophorin II to the endoplasmic reticulum involves both its transmembrane and cytoplasmic domains. Eur. J. Cell Biol. **79:**219–228.
16. **Guerin, J. L., J. Gelfi, C. Camus, M. Delverdier, J. C. Whisstock, M. F. Amardeihl, R. Py, S. Bertagnoli, and F. Messud-Petit.** 2001. Characterization and functional analysis of Serp3: a novel myxoma virus-encoded serpin involved in virulence. J. Gen. Virol. **82:**1407–1417.
17. **Haque, M., J. Chen, K. Ueda, Y. Mori, K. Nakano, Y. Hirata, S. Kanamori, Y. Uchiyama, R. Inagi, T. Okuno, and K. Yamanishi.** 2000. Identification and analysis of the K5 gene of Kaposi's sarcoma-associated herpesvirus. J. Virol. **74:**2867–2875.
18. **Ishido, S., J. K. Choi, B. S. Lee, C. Wang, M. DeMaria, R. P. Johnson, G. B. Cohen, and J. U. Jung.** 2000. Inhibition of natural killer cell-mediated cytotoxicity by Kaposi's sarcoma-associated herpesvirus K5 protein. Immunity **13:**365–374.
19. **Ishido, S., C. Wang, B. S. Lee, G. B. Cohen, and J. U. Jung.** 2000. Downregulation of major histocompatibility complex class I molecules by Kaposi's sarcoma-associated herpesvirus K3 and K5 proteins. J. Virol. **74:**5300–5309.
20. **Jackson, M. R., T. Nilsson, and P. A. Peterson.** 1990. Identification of a consensus motif for retention of transmembrane proteins in the endoplasmic reticulum. EMBO J. **9:**3153–3162.
21. **Kruse, N., and O. Weber.** 2001. Selective induction of apoptosis in antigen-presenting cells in mice by Parapoxvirus ovis. J. Virol. **75:**4699–4704.
22. **Lee, H. J., K. Essani, and G. L. Smith.** 2001. The genome sequence of yaba-like disease virus, a yatapoxvirus. Virology **281:**170–192.
23. **Le Gall, S., L. Erdtmann, S. Benichou, C. Berlioz-Torrent, L. Liu, R. Benarous, J. M. Heard, and O. Schwartz.** 1998. Nef interacts with the mu subunit of clathrin adaptor complexes and reveals a cryptic sorting signal in MHC I molecules. Immunity **8:**483–495.
24. **Lehner, P. J., J. T. Karttunen, G. W. Wilkinson, and P. Cresswell.** 1997. The human cytomegalovirus US6 glycoprotein inhibits transporter associated with antigen processing-dependent peptide translocation. Proc. Natl. Acad. Sci. USA **94:**6904–6909.
25. **Liu, G., L. Thomas, R. A. Warren, C. A. Enns, C. C. Cunningham, J. H. Hartwig, and G. Thomas.** 1997. Cytoskeletal protein ABP-280 directs the intracellular trafficking of furin and modulates proprotein processing in the endocytic pathway. J. Cell Biol. **139:**1719–1733.
26. **Marck, C.** 1988. 'DNA Strider': a 'C' program for the fast analysis of DNA and protein sequences on the Apple Macintosh family of computers. Nucleic Acids Res. **16:**1829–1836.
27. **Massung, R. F., V. Jayarama, and R. W. Moyer.** 1993. DNA sequence analysis of conserved and unique regions of swinepox virus: identification of genetic elements supporting phenotypic observations including a novel G protein-coupled receptor homologue. Virology **197:**511–528.
28. **McFadden, G., and K. Kane.** 1994. How DNA viruses perturb functional MHC expression to alter immune recognition. Adv. Cancer Res. **63:**117–209.
29. **Messud-Petit, F., J. Gelfi, M. Delverdier, M. F. Amardeilh, R. Py, G. Sutter, and S. Bertagnoli.** 1998. Serp2, an inhibitor of the interleukin-1β-converting enzyme, is critical in the pathobiology of myxoma virus. J. Virol. **72:**7830–7839.
30. **Nicholas, J., V. Ruvolo, J. Zong, D. Ciufo, H. G. Guo, M. S. Reitz, and G. S. Hayward.** 1997. A single 13-kilobase divergent locus in the Kaposi sarcoma-associated herpesvirus (human herpesvirus 8) genome contains nine open reading frames that are homologous to or related to cellular proteins. J. Virol. **71:**1963–1974.
31. **Pamer, E., and P. Cresswell.** 1998. Mechanisms of MHC class I-restricted antigen processing. Annu. Rev. Immunol. **16:**323–358.
32. **Parlato, S., A. M. Giammarioli, M. Logozzi, F. Lozupone, P. Matarrese, F. Luciani, M. Falchi, W. Malorni, and S. Fais.** 2000. CD95 (APO-1/Fas) linkage to the actin cytoskeleton through ezrin in human T lymphocytes: a novel regulatory mechanism of the CD95 apoptotic pathway. EMBO J. **19:**5123–5134.
33. **Perkus, M. E., J. Tartaglia, and E. Paoletti.** 1995. Poxvirus-based vaccine candidates for cancer, AIDS, and other infectious diseases. J. Leukoc. Biol. **58:**1–13.
34. **Petit, F., S. Bertagnoli, J. Gelfi, F. Fassy, C. Boucraut-Baralon, and A. Milon.** 1996. Characterization of a myxoma virus-encoded serpin-like protein with activity against interleukin-1β-converting enzyme. J. Virol. **70:**5860–5866.
35. **Petit, F., C. Boucraut-Baralon, R. Py, and S. Bertagnoli.** 1996. Analysis of myxoma virus genome using pulsed-field gel electrophoresis. Vet. Microbiol. **50:**27–32.
36. **Romero, C. H., T. Barrett, S. A. Evans, R. P. Kitching, P. D. Gershon, C. Bostock, and D. N. Black.** 1993. Single capripoxvirus recombinant vaccine for the protection of cattle against rinderpest and lumpy skin disease. Vaccine **11:**737–742.
37. **Saha, V., T. Chaplin, A. Gregorini, P. Ayton, and B. D. Young.** 1995. The leukemia-associated-protein (LAP) domain, a cysteine-rich motif, is present in a wide range of proteins, including MLL, AF10, and MLLT6 proteins. Proc. Natl. Acad. Sci. USA **92:**9737–9741.
38. **Schwartz, O., V. Marechal, S. Le Gall, F. Lemonnier, and J. M. Heard.** 1996. Endocytosis of major histocompatibility complex class I molecules is induced by the HIV-1 Nef protein. Nat. Med. **2:**338–342.
39. **Theobald, M., J. Biggs, D. Dittmer, A. J. Levine, and L. A. Sherman.** 1995. Targeting p53 as a general tumor antigen. Proc. Natl. Acad. Sci. USA **92:**11993–11997.
40. **Tripathy, D. N.** 1999. Swinepox virus as a vaccine vector for swine pathogens. Adv. Vet. Med. **41:**463–480.
41. **Tulman, E. R., C. Afonso, Z. Lu, L. Zsak, G. F. Kutish, and D. L. Rock.** 2001. The genome of lumpy skin disease virus. J. Virol. **75:**7122–7130.
42. **Upton, C., J. L. Macen, and G. McFadden.** 1987. Mapping and sequencing of a gene from myxoma virus that is related to those encoding epidermal growth factor and transforming growth factor alpha. J. Virol. **61:**1271–1275.
43. **Upton, C., and G. McFadden.** 1986. Tumorigenic poxviruses: analysis of viral DNA sequences implicated in the tumorigenicity of Shope fibroma virus and malignant rabbit virus. Virology **152:**308–321.
44. **van Santen, V. L.** 1991. Characterization of the bovine herpesvirus 4 major immediate-early transcript. J. Virol. **65:**5211–5224.
45. **Virgin, H. W., IV, P. Latreille, P. Wamsley, K. Hallsworth, K. E. Weck, A. J. Dal Canto, and S. H. Speck.** 1997. Complete sequence and genomic analysis of murine gammaherpesvirus 68. J. Virol. **71:**5894–5904.
46. **Wiertz, E. J., T. R. Jones, L. Sun, M. Bogyo, H. J. Geuze, and H. L. Ploegh.** 1996. The human cytomegalovirus US11 gene product dislocates MHC class I heavy chains from the endoplasmic reticulum to the cytosol. Cell **84:**769–779.

47. **Willer, D. O., G. McFadden, and D. H. Evans.** 1999. The complete genome sequence of Shope (rabbit) fibroma virus. Virology **264:**319–343.

48. **Yuen, L., and B. Moss.** 1987. Oligonucleotide sequence signaling transcriptional termination of vaccinia virus early genes. Proc. Natl. Acad. Sci. USA **84:**6417–6421.

49. **Zuniga, M., H. Wang, M. Barry, and G. McFadden.** 1999. Myxoma virus abrogates cell-surface expression of MHC I by multiple mechanisms. *In* S. Jameel and L. P. Villareal (ed.), Second ICGEB-UCI Virology Symposium. Science Publishers, Inc., New Delhi, India.

50. **Zuniga, M. C., H. Wang, M. Barry, and G. McFadden.** 1999. Endosomal/lysosomal retention and degradation of major histocompatibility complex class I molecules is induced by myxoma virus. Virology **261:**180–192.